CONTROLLED ACCELERATION OF SUPERIMPOSED BESSEL BEAMS

A. DUDLEY[1], C. SCHULZE[2], F. S. ROUX[1], M. DUPARRÉ[2], AND A. FORBES[1]
[1]CSIR National Laser Centre, PO Box 395, Pretoria 0001, South Africa.
[2]Institute of Applied Optics, Friedrich Schiller University, Fröbelstieg 1, Jena 07743, Germany.

ABSTRACT

In this work we present a mechanism for generating superpositions of non-canonical, higher-order Bessel beams, which are characterized by the anisotropy of the optical vortex on the propagation axis, known as the morphology parameter. We implement a spatial light modulator (SLM) to create superimposed, non-canonical, higher-order Bessel beams and a CCD camera to investigate the propagation of the resulting field. It is already known that the intensity profile of the resulting field experiences an angular rotation. However, we show that by tuning the morphology parameter, the rate of rotation will change periodically as a function of the propagation distance. Apart from demonstrating the controlled angular acceleration of the resulting intensity profile, we also show the transfer of energy between accelerating and decelerating sections in the intensity profile.

THEORETICAL BACKGROUND

In this work we consider the superposition of two fields, each a superposition having opposite azimuthal indices (l and $-l$)

$$U_1(r,z) = \exp(i\beta_1 z)\left[\cos\left(\theta/2\right)\exp(il\phi) + \sin\left(\theta/2\right)\exp(-il\phi)\right]J_l(\beta_1 \tan(\gamma) r), \quad (1)$$

and

$$U_2(r,z) = \exp(i\beta_2 z)\left[\sin\left(\theta/2\right)\exp(il\phi) + \cos\left(\theta/2\right)\exp(-il\phi)\right]J_l(\beta_2 \tan(\gamma) r). \quad (2)$$

Here θ is the morphology parameter and describes the anisotropy of the optical vortex around the beam axis. The difference in the longitudinal scales is $\Delta\beta = \beta_2 - \beta_1$.

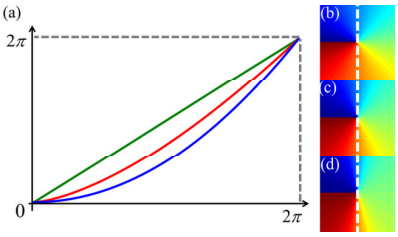

Fig. 1. (a) Plot of the azimuthal phase variation for the fields described in Eqs (1) and (2) for $\theta = 0$ (*green*), $\pi/5$ (*red*) and $\pi/3$ (*blue*). Examples of the azimuthal phase profiles for $l = 1$ and (b) $\theta = 0$, (c) $\theta = \pi/5$ and (d) $\theta = \pi/3$. Notice the variation in the azimuthal phase from linear to exponential.

The rotation rate of the resulting intensity profile is

$$\dot{\phi} = \frac{1}{2\pi}\tan^{-1}\left[\frac{\sin(\Delta\beta z)\cos(\theta)}{\cos(\Delta\beta z) + \sin(\theta)}\right]. \quad (3)$$

The inner part of the intensity profile will experience a fast angular rotation accompanied by a slow rotation in the outer part. When the rotation rate of the inner part of the intensity profile increases, the intensity is suppressed and the reverse occurs when the rotation rate decreases. The change in overall intensity of the two parts of the intensity profile are out of phase with one another. This is a consequence of energy conservation.

Consequently, the velocity and acceleration are

$$\dot{\phi} = \frac{\Delta\beta\cos(\theta)}{2l[1+\cos(\Delta\beta z)\sin(\theta)]}, \quad (4) \quad \text{and} \quad \ddot{\phi} = \frac{\Delta\beta^2\sin(\Delta\beta z)\sin(2\theta)}{4l[1+\cos(\Delta\beta z)\sin(\theta)]^2}. \quad (5)$$

EXPERIMENTAL SETUP

The experimental setup is depicted in Fig. 2 (a). An expanded HeNe laser beam was directed onto the liquid crystal display of a SLM were holograms representing Durnin's ring-slit aperture [1] were encoded with the use of amplitude modulation [2] an example of which is given in Fig. 2 (b). Two ring-slit apertures were used, each encoded with a non-canonical azimuthal phase variation of order l and $-l$ respectively, to produce a superposition of Eqs (1) and (2). The Fourier transform of the field at the plane of the hologram, at the focal plane after lens L, was magnified with a 10× objective and captured on a CCD camera. A propagation factor ($\exp(ik_z z)$) was encoded into the hologram [3] to investigate the propagation and consequently angular rotation and energy transfer of the resulting field.

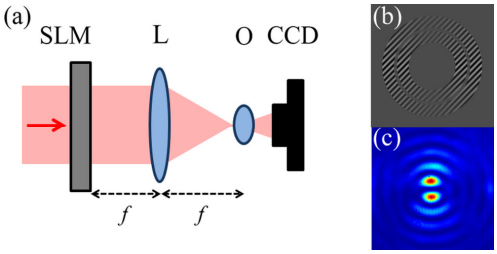

Fig. 2. (a) A schematic of the experimental setup for generating accelerating superimposed Bessel beams. (SLM: spatial light modulator; L: lens; O: objective; CCD: camera). (b) An example of the hologram encoded on the SLM ($l = 1$ and $\theta = \pi/3$) and the resulting field (c).

RESULTS AND DISCUSSION

The rotation rate of the intensity profile for superimposed fields for a range of azimuthal indices ($|l|$ = 1 to 6) were measured for an anisotropy of 0 ($\theta = 0$; linear). Examples of their intensity profiles are given in Fig. 3.

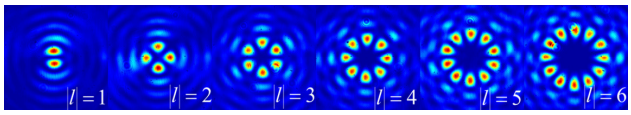

Fig. 3. The experimentally recorded intensity profiles recorded at the focal plane of lens L for a range of azimuthal indices $|l|$ = 1 to 6.

By increasing the anisotropy of the optical vortex (i.e. the morphology parameter θ) the rotation rate of the intensity profile increases in accordance with Eq. 3 and illustrated in Fig. 4.

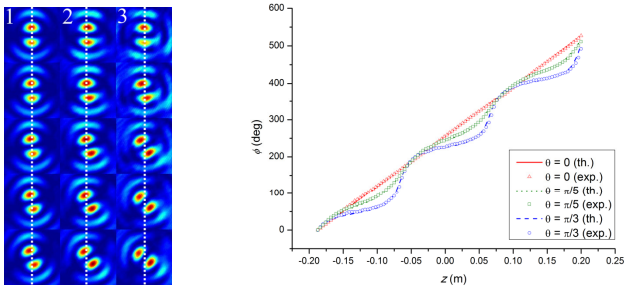

Fig. 4. Intensity profiles recorded at various propagation distances for a morphology parameter of θ = 0 (column 1), $\theta = \pi/5$ (column 2) and $\theta = \pi/3$ (column 3). Notice the location of the 'petal' is further away from the white dotted line as the morphology parameter increases. Plot of the angular rotation of the intensity profile as a function of the propagation distance z, for morphology parameters θ = 0, $\pi/5$ and $\pi/3$.

The derivative and double derivative of the rotation rate (Eq. (3)) determines the velocity (Eq. (4)) and acceleration (Eq. (5)) of the rotating 'petals' which are presented in Fig. 5. It is evident that the rotation rate of this field ($|l| = 1$ and $\theta = \pi/3$) accelerates and decelerates as it propagates.

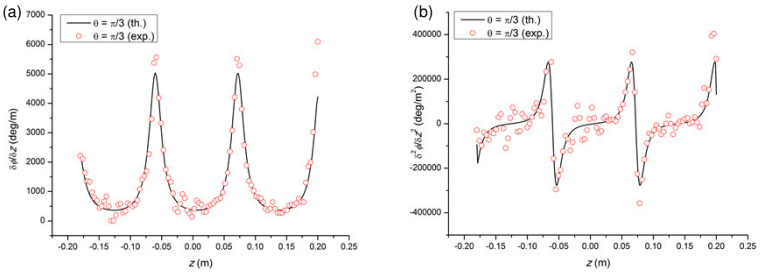

Fig. 5. (a) Graph of the velocity of the rotation rate as a function of the propagation distance z, for $|l| = 1$ and $\theta = \pi/3$. (b) Graph of the acceleration of the rotation rate as a function of the propagation distance z, for $|l| = 1$ and $\theta = \pi/3$

The intensity in the inner and outer sections of the intensity profile were monitored as the field propagates and the measurements are contained in Fig. 6, illustrating the transfer of energy between the two sections of the field.

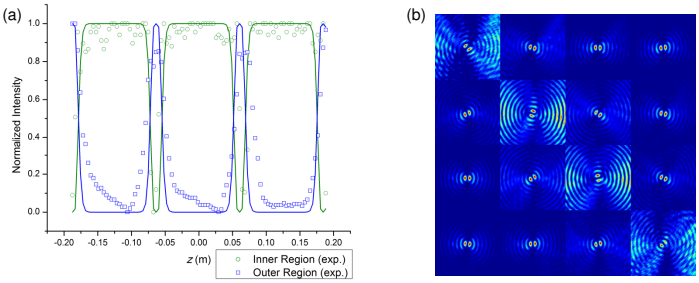

Fig. 6. (a) Graph of the maximum intensity in the centre (*green*) and outer (*blue*) regions of the intensity profile as a function of the propagation distance, z. (b) Snap-shots of the field recorded at intervals along the propagation distance.

REFERENCES

[1] J. Durnin, *et al*, Phys. Rev. Lett. 58, 1499 (1987).
[2] V. Arrizón, *et al*, J. Opt. Soc. Am. A 24(11), 3500-3507 (2007).
[3] C. Schulze, *et al*, Opt. Lett. 37(22), 4687-4689 (2012).